Available online at www.sciencedirect.com
SCIENCE DIRECT®
Journal of Power Sources 145 (2005) 1–9
JOURNAL OF POWER SOURCES
www.elsevier.com/locate/jpowsour

Li_2SO_4-based proton-conducting membrane for H_2S–air fuel cell

Guo-Lin Wei, Jing-Li Luo*, Alan R. Sanger, Karl T. Chuang, Li Zhong[1]

Department of Chemical and Materials Engineering, University of Alberta, Edmonton, Alta., Canada T6G 2G6

Received 17 October 2004; accepted 27 December 2004

Abstract

The composition and preparation procedure have been developed for a strong, integral Li_2SO_4-based gas-impermeable proton-conducting membrane. Incorporation of both Al_2O_3 and boric acid enhances mechanical and electrical properties. The membrane has been characterized using scanning electron microscope (SEM), energy dispersive X-ray (EDX) and electrochemical impedance spectrum (EIS) techniques. Use of the sodium salt of poly(acrylic acid) as an organic binder provided no improvement in membrane integrity, and caused severe Al_2O_3 segregation to the membrane surface. Addition of H_3BO_3 (2.5 or 5 wt.%) significantly improved membrane integrity and slightly decreased its electrical resistivity. The membrane is stable in H_2S–air fuel cell applications. There was no cross-over of H_2S through the improved membrane. Composite anodes based on metal sulfides had superior performance compared to Pt catalysts for conversion of H_2S. Membranes comprising 75–90 wt.% Li_2SO_4 and 10–25 wt.% Al_2O_3 to which 2.5–5.0 wt.% H_3BO_3 was added showed similar current–voltage and current–power performance, and had maximum current density about 40 mA cm^{-2} and maximum power density about 20 mW cm^{-2}.

Keywords: Fuel cell; Lithium sulfate membrane; Proton-conducting electrolyte; Boric acid; Hydrogen sulfide fuel; Composite sulfide anode catalyst

1. Introduction

H_2S is one of the most noxious, poisonous and abundant air pollutants, found in natural gas and several processing and other industrial effluent gas streams. It is converted to elemental sulfur using the Claus process. In the Claus process, the chemical energy of the oxidation reaction is either vented or partially recovered as low-grade steam. Fuel cell technology provides an economically and environmentally desirable alternative H_2S processing capability by generating high-grade electric power from the large amount of chemical energy associating with the oxidation of H_2S [1]. H_2S is converted with high selectivity to useful chemical raw materials, such as high-purity sulfur.

In 1987, Pujare et al. reported the first direct H_2S–air solid oxide fuel cell (SOFC) [1]. Oxygen is the preferred as cathode feed, but is more expensive than air. Since then, efforts have been directed toward improvement of cell performance [2–11]. A preferred electrolyte is oxide ion-conducting yttria-stabilized zirconia (YSZ), the characteristics of which are well known from use in SOFC for H_2-air fuel cells. Either Pt [3–5,8–11] or strontium-doped lanthanum manganite (LSM) [1,2,6] is used as cathode catalyst. Although Pt has been used as anode catalyst, it degraded quickly in a high-temperature H_2S atmosphere. Currently, it is generally accepted that the choice of anode materials is limited primarily to metal sulfides, such as thiospinels [1,2], WS_2 [2,6], $CoS_{1.035}$ [6], or $Li_2S/CoS_{1.035}$ [6]. High-performance composite metal sulfide-based anodes for H_2S–air SOFC were developed recently in our laboratories. In particular, it was shown that a composite Ni–Mo–S catalyst derived from MoS_2 and NiS [12], admixed with YSZ as ionic conductor and Ag as electronic conductor, had good performance and durability [11]. Using this composite anode and a 0.2 mm thick YSZ membrane, a current density of 820 mA cm^{-2} was obtained at 235 mV and the maximum power density was over 200 mW cm^{-2} at 0.77 V [11].

* Corresponding author. Tel.: +1 780 492 2232; fax: +1 780 492 2881.
E-mail address: jingli.luo@ualberta.ca (J.-L. Luo).
[1] Visiting Professor from South China University of Technology, Guangzhou, PR China.

0378-7753/$ – see front matter © 2005 Elsevier B.V. All rights reserved.
doi:10.1016/j.jpowsour.2004.12.015

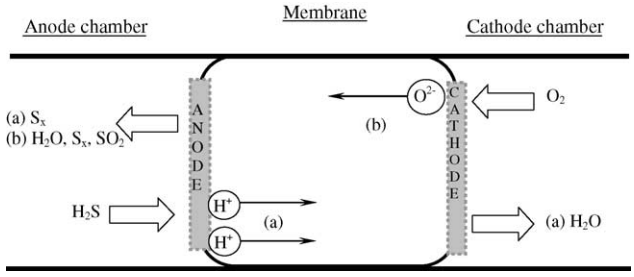

Fig. 1. Electrochemical processes in H_2S–air fuel cells. (a) Proton-conducting membrane; (b) oxide ion-conducting membrane.

The nature of the membrane determines the manufacturing requirements and mode of operation of conventional H_2-air fuel cells, and this is also true for H_2S–air fuel cells. The ions (H^+; O^{2-}) conducted within the membrane determine the electrochemical processes occurring in the fuel cell, as shown in Fig. 1 and Table 1. When proton-conducting membranes are used in an H_2S–air fuel cell, high-purity sulfur is the only product obtained in the anode chamber and water is the only product formed in the cathode chamber. With oxide ion-conducting membranes, elemental sulfur, H_2O and SO_2 are formed in the anode chamber, thus requiring further processing of the stream to remove SO_2.

Both oxide ion-conducting and proton-conducting membranes have been used in previous laboratory H_2S–air fuel cells. Pujare et al. used calcia-stabilized zirconia as well as YSZ as electrolyte [2]. Kirk and Winnick investigated the performance of cells using yttria- or samaria-doped ceria (oxide ion-conducting) or ytterbia-doped strontium cerate (proton-conducting) as membranes [3]. Peterson and Winnick reported the use of Li_2SO_4 as proton-conducting electrolyte material in H_2S–air fuel cells, and achieved a maximum short-circuit current density of 12 mA cm^{-2} at 725 °C [4]. Ytterbia-doped strontium cerate ($SrCe_{0.95}Yb_{0.05}O_3$) is a potentially useful proton-conducting electrolyte for H_2S–air fuel, but it converts to non-conductive $SrSO_4$ with time on stream [4]. In contrast, Li_2SO_4 is a stable proton-conductor for H_2S–air fuel cells [7]. X-ray diffraction (XRD) analysis of Li_2SO_4 membrane showed no change in composition of the membrane over time on stream [3]. However, Li_2SO_4 membranes are fragile and friable.

The most challenging task for development of H_2S–air fuel cells using a proton-conducting membrane is development of a membrane with chemical/thermal stability, mechanical strength, electrical conductivity and gas-impermeability. Currently, no such membrane is commercially available. We will now show that addition of boric acid to a Li_2SO_4–Al_2O_3 proton-conducting membrane greatly improves membrane integrity without compromising electrical performance. Independent studies have shown that membranes of the present composition are proton-conductors, using hydrogen concentration cell techniques [13,14]. Fuel-cell performance with the widely reported Pt anode catalyst will be compared to performance using metal sulfide-based composite anodes.

2. Experimental

2.1. Preparation of membranes

To prepare a membrane with a designed composition, the appropriate amount of Li_2SO_4 (and H_3BO_3, when needed) was weighed and mixed with water. The amount of water was insufficient to effect total dissolution. The complementary amount of Al_2O_3 was added, and the mixture then was mixed well to form a paste. The paste was dried in air, then ground to powder until the particle size was smaller than 75 μm. An aliquot of the powder was weighed (~1–1.5 g), loaded into a 2.54 cm die, and then compressed for about 0.5 h under 30 t pressure to form a wafer. The wafer so obtained was heated in air in an oven, first at 105 °C for 30–60 min and then at 800 °C for 360 min. The weight of the wafer was approximately 10 wt.% less than the initial weight of products, due to emission of water.

Wafers were also prepared using 1–2 wt.% of poly(acrylic acid, sodium salt) (MW = 2100) as an organic binder which was added to the Li_2SO_4–water paste. The binder was burned out completely when heating the wafers in air. The resulting membranes were porous, and were gas permeable.

Table 1
Electrochemical reactions in H_2S–air fuel cells with different membranes

Electrolyte type	Anode reaction(s)	Electrolytic conduction	Cathode reaction	Overall cell reaction(s)
(a) Proton-conducting	$H_2S - 2e^- \rightarrow 2H^+ + 1/2S_2$ (1)	Protons (H^+) transfer from anode side to cathode side	$O_2 + 4H^+ + 4e^- \rightarrow 2H_2O$ (7)	$2H_2S + O_2 \rightarrow 2H_2O + 1/2S_2$ (9)
	$H_2 - 2e^- \rightarrow 2H^+$ (2)[a]			$2H_2 + O_2 \rightarrow 2H_2O$ (10)[a]
(b) Oxide ion-conducting	$H_2S + 2O^{2-} - 6e^- \rightarrow 2H^+ + SO_2$ (3)	Oxide ions (O^{2-}) transfer from cathode side to anode side	$O_2 + 4e^- \rightarrow 2O^{2-}$ (8)	$2H_2S + 3O_2 \rightarrow 2H_2O + 2SO_2$ (11)
	$H_2S + O^{2-} - 2e^- \rightarrow H_2O + 1/2\ S_2$ (4)			$2H_2S + O_2 \rightarrow 2H_2O + 1/2S_2$ (9)
	$2H_2S + SO_2 \rightarrow 2H_2O + 3/2S_2$ (5)			$2H_2 + O_2 \rightarrow 2H_2O$ (10)[a]
	$H_2 + O^{2-} - 2e^- \rightarrow H_2O$ (6)[a]			

[a] H_2 results from the internal reforming of H_2S at temperatures in excess of 700 °C according to the following reaction: $H_2S\,(g) \Leftrightarrow H_2\,(g) + 1/2S_2\,(g)$ (12).

Membranes having a range of compositions have been prepared. The weight ratio of Li_2SO_4 to Al_2O_3 was normally selected to be either 90:10 or 75:25. No significant advantage was found from use of alternative ratios:

(1) Pure Li_2SO_4.
(2) 90 wt.% Li_2SO_4 + 10 wt.% Al_2O_3.
(3) 98–99 wt.% $(0.9Li_2SO_4 + 0.1Al_2O_3)$ + 1–2 wt.% poly (acrylic acid, sodium salt) (MW = 2100).
(4) 95 wt.% $(0.9Li_2SO_4 + 0.1Al_2O_3)$ + 5 wt.% H_3BO_3.
(5) 97.5 wt.% $(0.9Li_2SO_4 + 0.1Al_2O_3)$ + 2.5 wt.% H_3BO_3.
(6) 95 wt.% $(0.75Li_2SO_4 + 0.25Al_2O_3)$ + 5 wt.% H_3BO_3.

Wafers to be used as electrolyte disks were first checked for possible pinholes and cracks using an optical microscope. Only disks with no visibly discernable defects were used.

All chemical materials used in this work were obtained from Alfa-Aesar, except as otherwise indicated.

2.2. Characterization of membranes

Morphologies of the membranes were studied in detail with SEM and EDX techniques using a Hitachi S-2700 scanning electron microscope and PGT Imix system with a PRISM IG.

Pt paste was applied on both sides of membranes to be used to measure membrane electrical resistivity, and the assembly then was heated in air at 750 °C for 30 min. After the membrane had been slowly cooled to room temperature, it was installed in the fuel cell test station according to the same procedure as in fuel cell tests (see below). Pt contacting leads were attached to the Pt electrodes of the membrane. The resistivity of each membrane was measured at selected temperatures (450–675 °C). The temperature of the membrane was adjusted (either increased or decreased) at 5 °C min^{-1} to minimize thermal shock. After a selected temperature had been maintained for 30 min, resistivity data were acquired using conventional EIS methodology (see below).

2.3. Preparation of PEN (positive-electrolyte-negative) assemblies

To prepare a PEN assembly, Pt paste (Heraeus CL11-5100) was screen-printed first onto one side of the membrane. The assembly was then put in an oven and heated in air, first at 230 °C for 30 min and then at 750 °C for 30 min. The assembly was cooled slowly to room temperature. Then the anode catalyst in paste form was screen-printed onto the other side of the membrane. The whole assembly was then put in the oven and heated in nitrogen atmosphere, first at 230 °C for 30 min and then at 750 °C for 30 min. The PEN assembly was then cooled to room temperature slowly under nitrogen.

The anode materials used were Pt and a Ni–Mo–S composite catalyst [11]. Pt was applied as Pt paste (Heraeus CL11-5100). The metal sulfide-based composite anode was prepared from 95 wt.% Ni–Mo–S (prepared from MoS_2 + NiS, 1:1 weight ratio) and 5 wt.% Ag. A paste was prepared by dispersing the anode materials in α-terpineol. The paste was converted into the catalytic anode by sequentially applying the paste to the anode side of membrane, drying the paste on membrane, heating to 800 °C in nitrogen for 30 min, and cooling the assembly slowly to room temperature.

2.4. Installation of PEN assemblies into the fuel cell test station

A fuel cell test station similar to that shown in Ref. [8] was constructed, with some minor modifications that did not alter the principals of operation. To install the PEN assembly (2.54 cm diameter) into a test fuel cell, first the cathode side of the assembly was attached to a supporting annular alumina disk 3.2 cm in diameter and 0.3 cm in thickness using ceramic sealant (Aremco 503). An opening 1.1 cm in diameter in the center of the supporting ceramic disk allowed air to access the cathode. The combination so made was then sealed with ceramic sealant (Aremco 503) between two alumina tubular chambers (outer dimension 2.54 cm, length 40 cm), as described in Ref. [8]. An additional 3 mm wide sealant layer was applied around the sealing area to ensure a good seal. Platinum mesh was used as current collectors. The mesh surface was refreshed in the flame of a gas lamp prior to installation for each experiment [10]. The cell was then heated in a tubular furnace (Thermolyne F79300), with nitrogen passing through the anode chamber and air through the cathode chamber. To cure the sealant, the furnace temperature was increased at 0.8 °C min^{-1} to 230 °C, and held at that temperature for 1 h. The temperature then was increased to a selected testing temperature, typically 600 °C, and held at that temperature for the duration of each set of tests.

2.5. Measurement of H_2S–air fuel cell performance

Cell performance was determined using pure H_2S as the anode feed. The cell open circuit voltage (OCV) was monitored as a function of time on stream. Data were recorded with a Gamry electrochemical measurement system (PC4-750). Initial electrical performance data were evaluated to determine cell integrity. Typically, a cell that had no leaks showed a steady OCV value after about 30 min. An OCV that fluctuated, or that had a persistently low value (0.5–0.6 V), indicated possible leaks in the cell, and no further tests were conducted using that PEN assembly.

After a steady OCV was achieved, EIS measurements were performed to determine cell resistance. The frequency region was 0.2–100,000 Hz and a stimulating AC signal of 5 mV was imposed onto OCV. Potentiodynamic measurements were conducted to determine the cell current–voltage performance in the IR compensation mode using the Gamry system at a scanning rate of 1 mV s^{-1} [10].

2.6. Stability of Li_2SO_4 in membranes under operating conditions

Li_2SO_4 was reduced when heated in an atmosphere of H_2 under operating conditions for a H_2–O_2 fuel cell [15]. The products were Li_2S and LiOH. Consequently, we evaluated the stability of Li_2SO_4 in the present membranes under H_2S–O_2 fuel cell operating conditions. XRD were obtained for a fresh membrane and one operated for 5 h at 700 °C. In addition, a membrane comprising the electrolyte alone, without electrodes, was heated to 700 °C in pure H_2S for 7.5 h, and XRD of the fresh and treated samples were compared. In neither case was any evidence found for formation of either Li_2S or LiOH, showing that Li_2SO_4 is stable in an atmosphere of H_2S, in agreement with the findings of Peterson and Winnick [4].

3. Results and discussion

3.1. Method of membrane preparation

Several proton-conducting membranes have been prepared based on Li_2SO_4. However, it was found to be very difficult to obtain an integral wafer by pressing Li_2SO_4 alone. These membranes were very powdery after being heated in air. Particles adhered to each other loosely and were easily abraded from the membrane.

Proton-conducting membranes with improved mechanical and electrical properties have been prepared using a mixture of Li_2SO_4 and Al_2O_3 [7,16,17]. However, it remained difficult to prepare integral membranes by pressing a mixture of Li_2SO_4 and Al_2O_3 alone. We have now found that addition of 2.5–5 wt.% boric acid to a Li_2SO_4–Al_2O_3 mixture greatly enhanced the integrity of the electrolyte wafer. A key factor appeared to be that the water content in the mixture powder that could be lost on heating the wafer was about 10 wt.%, but the reason for this amount is not presently known.

Membranes containing different ratios of Li_2SO_4 and Al_2O_3 obtained after a single pressing and heating sequence had similar membrane morphology. They were all fragile and very porous. Powder was found to detach easily from each membrane. Optical microscopic inspection indicated loose adherence between particles, and many cavities were found on the membrane surface. SEM images (Section 3.2) confirmed these observations. The membranes were sufficiently porous to allow H_2S cross-over. Thus a process comprising a single cycle of mixing, grinding, pressing and heating did not enable manufacture of membranes with an appropriate microstructure to prevent gas permeability, and the low-density membranes so made were not structurally sound. It was found that a procedure comprising mixing, drying and then a repeated sequence of grinding, pressing and heating (3–5 times) afforded a more dense membrane. Similar procedures with two cycles of the sequence have been described elsewhere [4,18].

In the repeated grinding, pressing and heating procedure, a Li_2SO_4–Al_2O_3 membrane prepared as above was ground again until the particle size was less than 75 μm. The resulting powder was wetted again by standing in a humidified atmosphere until the weight gain was around 10 wt.% of the final weight. The resulting powder was then pressed and heated again to form a second wafer. Optical microscopic inspection confirmed an improvement in the membrane morphology with denser structure and less loose particles or cavities on the surface. The procedure was repeated up to five times, after which no further benefit accrued.

Although fuel cell performance was improved when using a membrane prepared from repeatedly ground, pressed and heated material, the repetitive procedure was time-consuming. Consequently, two alternative approaches were tried in attempts to find a more efficient procedure for preparing dense and strong membranes. In one approach, the sodium salt of poly(acrylic acid) (1–1.8 wt.%) was used as binder in the mixture of Li_2SO_4 and Al_2O_3. Use of the binder made it easier to obtain an integral membrane wafer by pressing. However, during heat-treatment, the binder was destroyed by oxidation in air, and this left voids in the material. Readily detachable powder was again observed on the membrane surface. SEM showed enlarged particles and cavities (see below). Thus use of polymer binder did not improve the integrity or stability of the resulting membrane, and the membrane was porous.

In another approach, H_3BO_3 (2.5 or 5 wt.%) was incorporated as a well-dispersed additive throughout the Li_2SO_4–Al_2O_3 mixture before pressing and heating the mixture. The mechanical and electrical properties of the resulting membrane were significantly improved by the addition of H_3BO_3. No loose particles or cavities were observed on the membrane surface using optical microscopy, although a small fraction was observed with SEM. The membranes were rigid and strong, and easy to handle in PEN fabrication and fuel cell testing. No H_2S cross-over to the air chamber was observed during fuel cell testing. Performance of membranes incorporating H_3BO_3 was similar to that for those made using the re-grinding and reheating procedure. Thus, H_3BO_3 is a promising additive for the preparation of high-performance membranes.

3.2. Morphologies of membranes

Following preliminary inspection of membranes with optical microscopy, the membrane morphology was investigated further with SEM and EDX techniques. A SEM image of a membrane prepared from a binary mixture of Li_2SO_4 and Al_2O_3 is shown in Fig. 2A. Cavities pervaded throughout the membrane, and many cracks were seen on the surface.

Table 2 shows the elemental atomic proportions on various membrane surfaces. Since light elements such as Li and B cannot be analyzed with EDX technique, only results for ratios of Al, S and O are shown. Compared with the com-

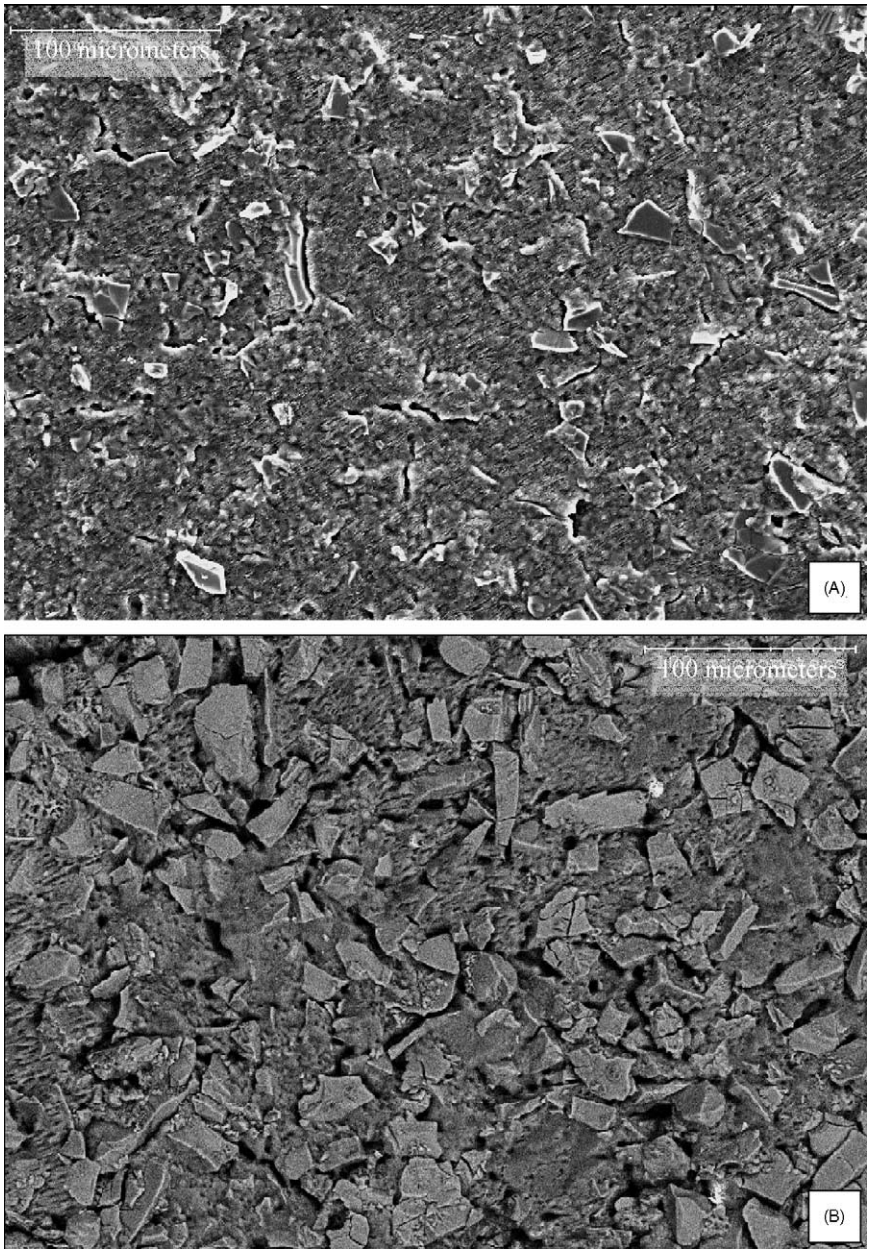

Fig. 2. SEM images of 90 wt.% Li_2SO_4 + 10 wt.% Al_2O_3 membrane after heat-treatment in air. (A) Without organic binder; (B) with organic binder.

position of the bulk of the membrane prepared from Li_2SO_4 and Al_2O_3 alone, the overall Al surface proportion for the membrane was up to twice as high as the bulk proportion of Al, and that of S was very close to the bulk proportion. EDX results in Table 2 also indicated that the matrix, as indicated by the membrane surface after excluding loose particles, comprised mainly Li_2SO_4 (S/O = 0.310), and that the Al_2O_3 content was very low (Al/O = 0.002). Meanwhile the particles contained virtually no sulfate (S/O = 0.002). In combination, these results implied segregation and accumulation of Al on the membrane surface, and therefore separation, rather than integration, of Li_2SO_4 and Al_2O_3 in the membrane.

Fig. 2B shows a SEM photograph of the membrane prepared from the Li_2SO_4–Al_2O_3 mixture when using the sodium salt of poly(acrylic acid) as an organic binder. Enlarged particles, cavities and boundary gaps are clearly visible. The amount of particles was increased greatly when compared with the membrane prepared using no organic binder, and these particles adhered very loosely to each other. No improvement was observed in membrane morphology when compared to a membrane prepared without binder. EDX results (Table 2) again indicated that the surface particles comprised mainly Al_2O_3 and that the matrix comprised mainly Li_2SO_4. The overall Al surface proportion was nearly five times higher than that of the bulk

Table 2
Elemental atomic compositions of membrane surfaces as determined using EDX[a]

Membrane, 90 wt.% Li_2SO_4 + 10 wt.% Al_2O_3	Analysis area	Atomic proportions	
		Al/O	S/O
No binder[b]	Bulk, calculated	0.055	0.229
	Overall surface	0.126	0.296
	Matrix	0.002	0.310
	Particle	0.988	0.002
+Binder[c]	Bulk, calculated	0.055	0.229
	Overall surface	0.464	0.222
	Matrix	0.002(5)	0.309
	Particle	0.971	<0.001
+5 wt.% H_3BO_3[d]	Bulk, calculated	0.051	0.214
	Overall surface	0.031	0.373
	Area 1 (particle)	1.019	0.019
	Area 2 (particle)	0.037	0.335
	Area 3	<0.001	0.487
+2.5 wt.% H_3BO_3[e]	Bulk, calculated	0.053	0.222
	Overall surface	0.047	0.388
	Area 1 (particle)	0.868	0.006
	Area 2	0.010	0.423

[a] Atomic percentage for O, Al, S only; Li, B are not detected using EDX (n.d.: not detected).
[b] See Fig. 2A for the corresponding SEM photo.
[c] See Fig. 2B for the corresponding SEM photo.
[d] See Fig. 3A for the corresponding SEM photo and the analysis area explication.
[e] See Fig. 3B for the corresponding SEM photo and the analysis area explication.

composition, which showed significant segregation of Al to the surface, consistent with the increase in the amount of Al_2O_3 particles seen on the membrane surface.

Addition of H_3BO_3 to the powdered mixture used to prepare the membranes resulted in significantly improved integration of Li_2SO_4 and Al_2O_3 in the resulting membrane. Fig. 3A shows the SEM image of the membrane containing 5 wt.% H_3BO_3. The membrane showed a more strongly integrated surface, although cracks and some adhering particles could still be seen, which indicated a need for further improvement in the membrane preparation method. As shown by EDX results (Table 2), the overall surface proportion of Al was close to that of the bulk composition, while the surface proportion of S was slightly higher than that of the bulk. The composition of the general surface consisted mainly of Li_2SO_4 (Area 3, Fig. 3A). Some particles consisted mainly of Al_2O_3 combined with a lesser amount of Li_2SO_4 (Area 1, Fig. 3A), and others contained mainly Li_2SO_4 and some Al_2O_3 (Area 2, Fig. 3A). Similar results were obtained for the membrane containing 2.5 wt.% H_3BO_3 (Fig. 3B and Table 2), except that a small number of cavities were found on the membrane surface.

3.3. Electrical conductivity of membranes

EIS technique was used to study the change in the membrane electrical conductivity with temperature. Fig. 4 shows the conductivity as a function of temperature for membranes with different H_3BO_3 proportion: 0, 2.5 and 5 wt.%. A small increase in electrical conductivity occurred as a result of incorporation of H_3BO_3. An abrupt change in the cell conductivity occurred around 575 °C, the temperature of which was the same for each membrane, with or without H_3BO_3 (Fig. 4). Conductivity increases little with temperature above 575 °C. Below 575 °C, it decreases dramatically. This indicates that 575 °C is the lowest operating temperature appropriate for the present Li_2SO_4-based proton-conducting membranes. This phenomenon is attributed to the Li_2SO_4 phase transformation known to occur at 577 °C [4]. Li_2SO_4 is in the cubic α-phase above 577 °C, which has high proton conductivity, and in the monoclinic β-phase below 577 °C, which has low proton conductivity, as described by Peterson and Winnick [4]. As seen in Fig. 4, a hysteresis phenomenon was observed around 575 °C with increasing temperature while no such phenomenon was observed with decreasing temperature. The hysteresis implied a slower transformation rate from β-phase to α-phase while the reverse process was relatively rapid.

3.4. Fuel cell performance

Baseline tests were run with membranes prepared from Li_2SO_4 alone. Solid sulfur was found in the cathode chamber after the cell had been cooled to room temperature, indicating that H_2S had crossed over through the membrane. Current densities were low and close to reported values for a different membrane [4], and disrupted *I–V* curves were obtained.

Further tests then were run with Li_2SO_4-based proton-conducting membranes that contained other additives. Current–voltage (Fig. 5) and current–power (Fig. 6) performance were determined for each of various membranes used in the preparation of PEN assemblies.

3.4.1. Comparison of anode catalysts

Both Pt [3–5] and the composite material derived from (Ni–Mo–S + Ag) [10] have been used as starting materials for anodes in H_2S–air fuel cells, mainly with oxide ion-conducting membranes. To compare their performances in H_2S–air fuel cells using Li_2SO_4-based proton-conducting electrolytes, membranes were prepared from wafers prepared by doubly grinding, pressing and heating the material prepared from the mixture (90 wt.% Li_2SO_4 + 10 wt.% Al_2O_3). Figs. 5 and 6 compare the performances for fuel cells with Pt and metal sulfide-based composite anodes. Both cells showed very similar performance with maximum current density about 20 mA cm^{-2} and maximum power density around 9 mW cm^{-2}. However, the metal sulfide-based composite anode was more stable than Pt over time on stream. Pt reversibly formed PtS in high-temperature H_2S atmosphere, leading to its delamination from the membrane during cell operation, as was previously observed also for solid oxide membranes [5,8,9]. The metal sulfide-based composite anodes did not delaminate. Another advantage of using the metal sulfide-based composite anode is that it is possible, by adjusting the

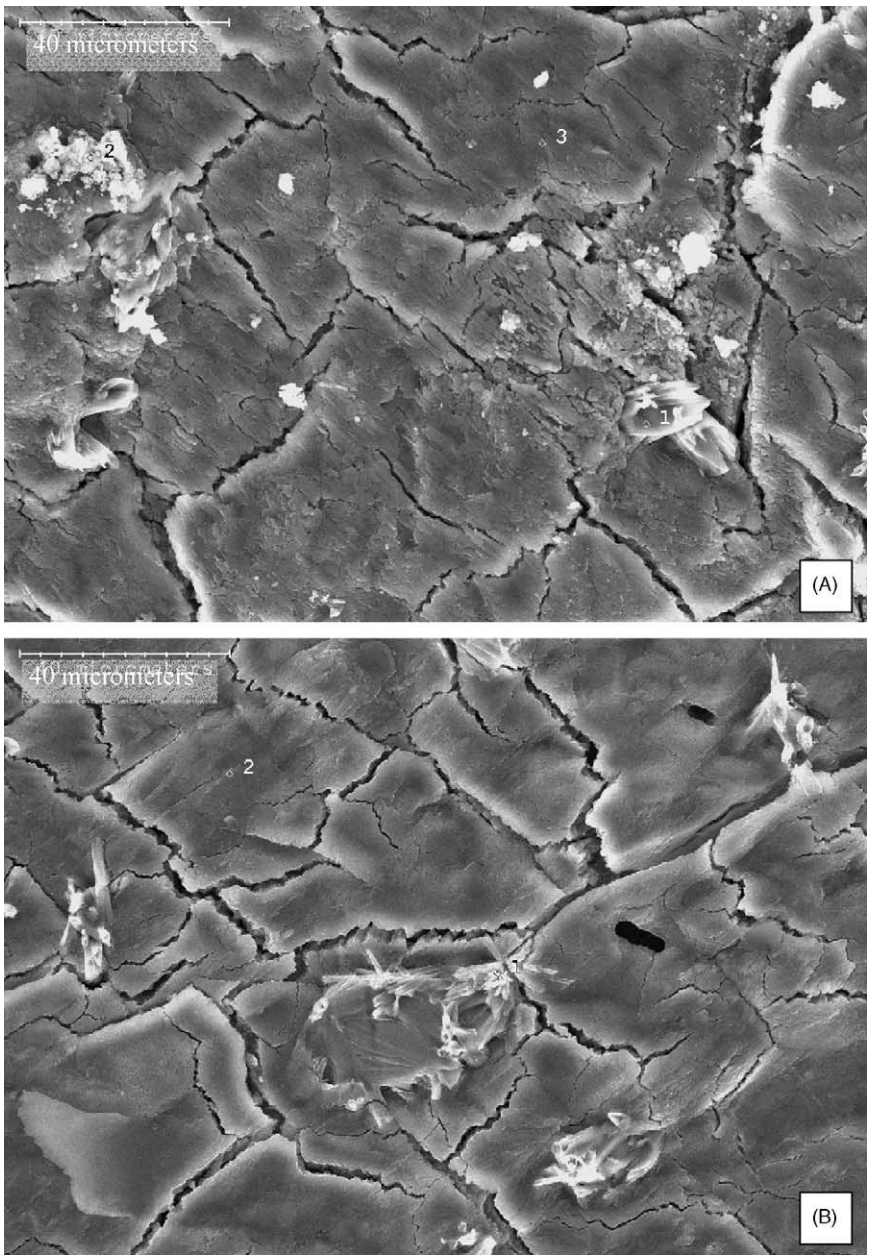

Fig. 3. SEM images of membrane after heat-treatment in air: (A) 95 wt.% $(0.9Li_2SO_4 + 0.1Al_2O_3) + 5$ wt.% H_3BO_3; (B) 97.5 wt.% $(0.9Li_2SO_4 + 0.1Al_2O_3) + 2.5$ wt.% H_3BO_3.

anode chemical composition, to tailor its activity and stability to the conditions of the system and its thermal compatibility with the membrane [10,11,19,20].

3.4.2. *Influence of membrane composition on fuel cell performance*

Fuel cell performances of different membranes were determined using the same composition for the metal sulfide-based composite anode (95 wt.% Ni–Mo–S + 5 wt.% Ag). Fuel cells using low-density Li_2SO_4–Al_2O_3 membranes, such as those obtained using a single sequence of mixing, grinding, pressing and heating, showed fluctuating and very low open circuit voltage and poor current–voltage/power performance. Sulfur deposits were found in the cathode (air) chamber after the cell was cooled down. These effects were caused by cross-over of H_2S, which lead to reaction with air in the cathode chamber. The Pt cathode also degraded in the presence of sulfur. Thus low-density membranes were unsuitable for use in H_2S–air fuel cells.

An improvement in H_2S–air fuel cell performance was achieved when using membranes comprising only Li_2SO_4 and Al_2O_3 by repeating the grinding–pressing–heating membrane preparation sequence several times. Figs. 7 and 8 show fuel cell performance using a membrane prepared by repeating the sequence three times. The maximum current density was approximately doubled to about 40 mA cm^{-2},

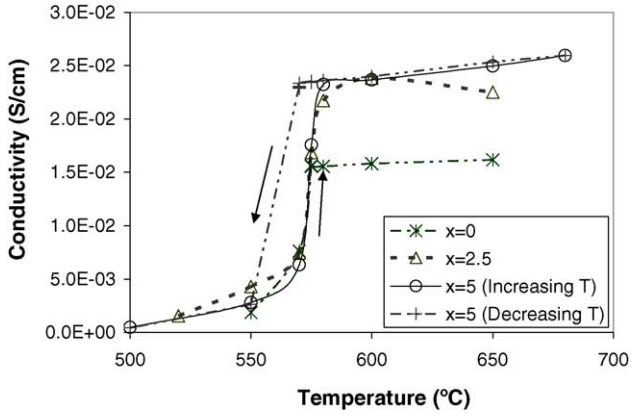

Fig. 4. Change of resistance/thickness with temperature. Electrolyte composition: $(100 - X)$ wt.% $(0.9Li_2SO_4 + 0.1Al_2O_3) + X$ wt.% H_3BO_3.

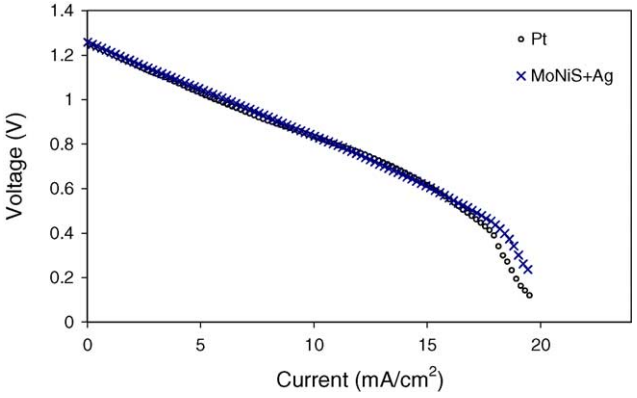

Fig. 5. Comparison of *I–V* performance for H_2S–air fuel cells with Pt or composite materials derived from (Ni–Mo–S + Ag) as anodes. Cathode: Pt; operating temperature: 650 °C. Flow rate – H_2S: 20 mL min^{-1}; air: 20 mL min^{-1}.

and the maximum power to about 20 mW cm^{-2}, when compared with the performance of a membrane prepared using doubly processed material (Figs. 5 and 6). Repeating the process steps appeared to improve both membrane structure by reducing the incidence of cavities, and electrical performance by improving interparticulate contacts in the membrane.

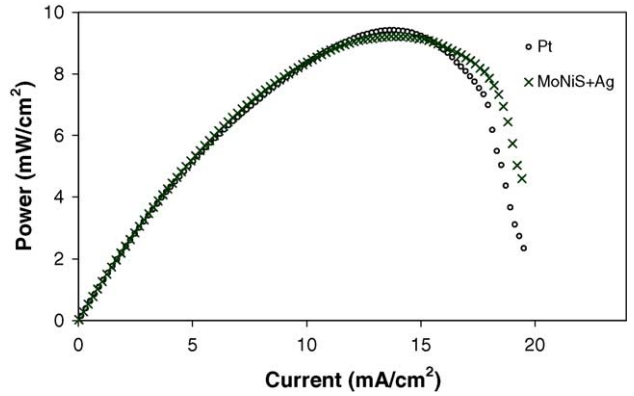

Fig. 6. Comparison of *I–P* performance for H_2S–air fuel cells with Pt or composite materials derived from (Ni–Mo–S + Ag) as anodes. Cathode: Pt; operating temperature: 650 °C. Flow rate – H_2S: 20 mL min^{-1}; air: 20 mL min^{-1}.

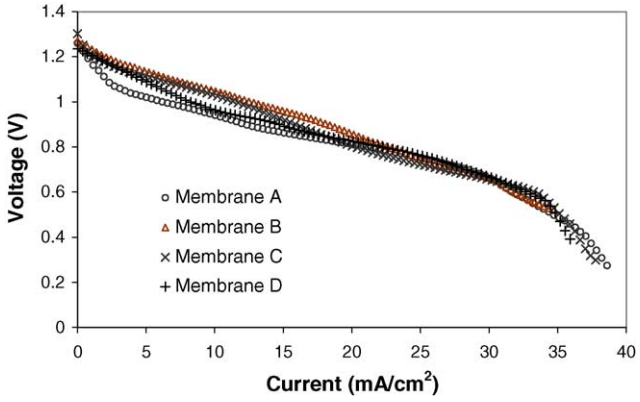

Fig. 7. *I–V* performance for H_2S–air fuel cells with different membranes. Anode: composite materials derived from (Ni–Mo–S + Ag). Cathode: Pt; operating temperature: 600 °C. Flow rate – H_2S: 20 mL min^{-1}; air: 20 mL min^{-1}.

Fuel cells having Li_2SO_4–Al_2O_3 membranes incorporating 2.5 or 5 wt.% H_3BO_3 prepared using only one pressing–heating sequence showed similar high performances (Figs. 7 and 8) to membranes with no H_3BO_3 that had been processed up to five times. No H_2S permeation through these membranes was observed during fuel cell tests. Thus a similar enhancement in performance was attained without the need for a repeated grinding–pressing–heating sequence. Three compositions of materials were used to prepare membranes installed in fuel cells: [95 wt.% $(0.9Li_2SO_4 + 0.1Al_2O_3)$ + 5 wt.% H_3BO_3], [97.5 wt.% $(0.9Li_2SO_4 + 0.1Al_2O_3)$ + 2.5 wt.% H_3BO_3], and [95 wt.% $(0.75Li_2SO_4 + 0.25Al_2O_3)$ + 5 wt.% H_3BO_3]. Fuel cells containing each of these membranes showed performances similar to that of a membrane comprising only Li_2SO_4 and Al_2O_3 that had been processed three times. The maximum power densities were each about 20 mW cm^{-2}, and the maximum current was around 40 mA cm^{-2}. The addition of 2.5–5.0 wt.% H_3BO_3 improved the mechanical properties of Li_2SO_4–Al_2O_3 composite membranes, allowed no cross-

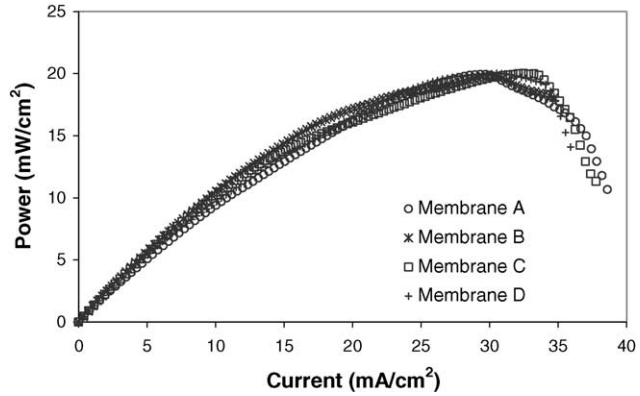

Fig. 8. *I–P* performance for H_2S–air fuel cells with different membranes. Anode: composite materials derived from (Ni–Mo–S + Ag). Cathode: Pt; operating temperature: 600 °C. Flow rate – H_2S: 20 mL min^{-1}; air: 20 mL min^{-1}.

over of H_2S, and did not compromise the electrochemical performance of the membranes.

4. Conclusions

Proton-conducting membranes comprising Li_2SO_4 and Al_2O_3 with 2.5 or 5.0 wt.% H_3BO_3 membranes had higher integrity and strength than membranes prepared without H_3BO_3, and had good electrical performance. The use of the sodium salt of poly(acrylic acid) as organic binder gave a porous and gas permeable membrane with poor integrity, cracks and cavities, with segregated Al_2O_3 particles loosely adhering to each other and to the membrane surface. Significant H_2S permeation was found for low-density membranes in a laboratory fuel cell. A process comprising mixing Li_2SO_4 and Al_2O_3 alone and then a repeated sequence of grinding, pressing and heating the resulting mixture afforded a membrane having increased density, improved mechanical integrity, and decreased H_2S permeability, but the process was time-consuming. Addition of H_3BO_3 to Li_2SO_4–Al_2O_3 mixtures before preparing the membrane provided the same benefits through a single process sequence. There was no Al segregation to form Al_2O_3 particles at the surface of membranes incorporating H_3BO_3, in contrast to membranes without H_3BO_3. H_2S did not permeate through H_3BO_3-containing membranes.

The membranes are stable during operation of H_2S–O_2 fuel cells, whereas they are unstable during operation of H_2–O_2 fuel cells

A Ni–Mo–S and Ag composite anode showed similar activity to Pt anodes. The Ni–Mo–S catalyst had higher stability than Pt catalyst during cell operation and, in contrast to Pt, did not delaminate from any of the electrolytes. Maximum power densities were about 20 mW cm^{-2} and maximum current densities were around 40 mA cm^{-2}.

References

[1] N.U. Pujare, K.W. Semkow, A.F. Sammells, J. Electrochem. Soc. 134 (1987) 2639.
[2] N.U. Pujare, K.J. Tsai, A.F. Sammells, J. Electrochem. Soc. 136 (1989) 3662.
[3] T.J. Kirk, J. Winnick, J. Electrochem. Soc. 140 (1993) 3494.
[4] D. Peterson, J. Winnick, J. Electrochem. Soc. 143 (1996) 55.
[5] D. Peterson, J. Winnick, J. Electrochem. Soc. 145 (1998) 1449.
[6] C. Yates, J. Winnick, J. Electrochem. Soc. 146 (1999) 2841.
[7] B. Zhu, S. Tao, Solid State Ionics 127 (2000) 83.
[8] M. Liu, P. He, J.-L. Luo, A.R. Sanger, K.T. Chuang, J. Power Sour. 94 (2001) 20.
[9] P. He, M. Liu, J.-L. Luo, A.R. Sanger, K.T. Chuang, J. Electrochem. Soc. 149 (2002) A808.
[10] G.-L. Wei, M. Liu, J.-L. Luo, A.R. Sanger, K.T. Chuang, J. Electrochem. Soc. 150 (2003) A463.
[11] K.T. Chuang, J.-L. Luo, G. Wei, A.R. Sanger, US Patent Application 20030215697 (2003).
[12] D.S. Thakur, P. Grange, B. Delmon, J. Catal. 91 (1985) 318.
[13] A. Lunden, B.-E. Mellander, B. Zhu, Acta Chem. Scand. 45 (1991) 981.
[14] J.-X. Li, G.-L. Wei, J. Melnik, J.-L. Luo, A.R. Sanger, K.T. Chuang, J. Power Sources (2005) submitted for publication.
[15] S. Tao, Z. Zhan, P. Wang, G. Meng, Solid State Ionics 116 (1999) 29.
[16] B. Zhu, Z.H. Lai, B.-E. Mellander, Solid State Ionics 70–71 (1994) 125.
[17] B. Zhu, K. Rundgren, B.-E. Mellander, Solid State Ionics 97 (1997) 385.
[18] B. Zhu, B.-E. Mellander, J. Power Sour. 52 (1994) 289.
[19] G.-L. Wei, J.-L. Luo, A.R. Sanger, K.T. Chuang, J. Electrochem. Soc. 151 (2004) A232.
[20] M. Liu, G.-L. Wei, J.-L. Luo, A.R. Sanger, K.T. Chuang, J. Electrochem. Soc. 150 (2003) A1025.